REDUCED KINEMATIC FORMULATION BASED ON THE STRONG DISCONTINUITY METHOD FOR REINFORCED CONCRETE COMPONENTS

E. KISHTA[*,a,b], B. RICHARD[a], C. GIRY[b] AND F. RAGUENEAU[b]

[a] CEA, DEN, DANS, DM2S, SEMT, Laboratoire d'Études de Mécanique Sismique
F-91191, Gif-sur-Yvette, France
[*]e-mail: ejona.kishta@cea.fr

[b]Laboratoire de Mécanique et Technologie de Cachan
ENS Cachan, CNRS, Université Paris-Saclay
61, avenue du Président Wilson, F-94235 Cachan Cedex, France

Key words: Quasi-brittle materials, Strong Discontinuity Approach, E-FEM, damage, Cast3M

Abstract. Damage models, developed in the last decades, insure a continuous description of the fracture process zone in quasi-brittle materials but fail at representing fine information of the cracking features such as openings and spacings. Recently, the concept of displacement discontinuities embedded into a standard finite element has been proved to be efficient in modeling fracture of quasi-brittle materials. The present paper aims at capturing crack openings in a natural way by using the Strong Discontinuity Approach (SDA). This later is coupled with a continuous anisotropic damage model accounting for different crack orientations and crack closure effects. A regularized version of the Dirac distribution and the hardening parameter provides+ the establishment of an enriched model compatible with the continuous one. Numerical simulations at the integration point level and a three-point bending test carried out on a single edge notched beam show the performances of the model.

1 INTRODUCTION

The complex behaviour of quasi-brittle materials has been widely studied. Quasi-brittle failure is characterized by an induced anisotropy : microcracks orientation is dependent on the loading path. Furthermore, different features such as cracking, crack closure effect and permanent strains are observed. Different approaches and models has been developed to capture the aforementioned features. Recent isotropic damage models, based on a continuum description of the media, succeed in representing the complex behavior of quasi-brittle materials. Nevertheless, cracking is described in a diffuse way and it is always difficult to quantify the cracking features such as openings and spacings without post-treatment methods [1]. Other approaches, like smeared-crack models, developed for concrete fracture, suffer from spurious stress transfer across an open crack (stress locking). This phenomenon is observed for fixed and rotating crack

334

models. For the first one, locking is due to shear stresses. For the second model, locking is due to the misalignment between the direction of the macroscopic crack and the finite element side [2]. Most of three-dimentionnal anisotropic models developed, using a tensorial variable, describe quite well global cracking, crack closure effects often by means of strain decomposition. However, several authors [3,4] have pointed out some problems when dealing with a spectral decomposition of the damage and strain tensors. In order to describe accurately the non-isotropic microcracking pattern, the anisotropic model needs to be simple and robust. For seismic applications, particularly for cyclic loadings, crack opening requirements induce the development of a numerical model which provides fine information (openings, spacings) in a natural way. The aim of our work is the development of an anisotropic damage model which enables crack openings explicitly and in a natural way.

Recently, embedded crack models, considering either elemental enrichment E-FEM [5] or nodal enrichment X-FEM [6] succed in describing fracture process zones in concrete. However, nodal enrichment is more time consuming, intrusive in a finite element code and has still to be improved in case of 3D problems. The Strong Discontinuity Approach (SDA) consists in a kinematically enhancement with a displacement jump leading to a singular strain field. Regularization technique of the singular strain field, performed on isotropic damage models or plasticity models, provides a discrete model compatible with the continuum one. In this paper, an anisotropic damage model, based on micromechanical assumptions, is used [7]. This model allows accounting for particular crack orientations and can represent either mode-I and mode-II cracking mechanisms which can be handled independently. The anisotropic damage model is then enriched using the SDA and the regularization technique is performed. A discrete constitutive model expressed in terms of a traction/separation law is obtained and applied to simple tests using a plate kinematic formulation.

The paper is organized as follows: in section 2, the anisotropic damage model used to describe concrete degradation with its associated constitutive relations, is described. The E-FEM framework and the regularization method for obtaining an enriched damage model are presented in section 3. Numerical implementation aspects are exposed in section 4. In section 5, the performance of the developed model is assessed by the analysis of a three-point bending test carried out on a single edge notched concrete beam.

2 CONTINUUM ANISOTROPIC DAMAGE MODEL

In this section, the anisotropic damage model is described. The definition of the damage state and the constitutive relations are exposed.

2.1 Damage definition

The model, based on micromechanical assumptions, describes the damage state (see figure 1) as the contribution of families of parallel cracks defined by a normal $\underline{n}_i$ and microcracking density ρ_i [7]. Damage is written as the couple ρ_i, $\underline{\underline{N}}_i$ where $\underline{\underline{N}}_i$ are directionnal tensors calculated as the tensorial product of normals to the crack $\underline{n}_i$.

$$\underline{\underline{N}}_i = \underline{n}_i \otimes \underline{n}_i \tag{1}$$

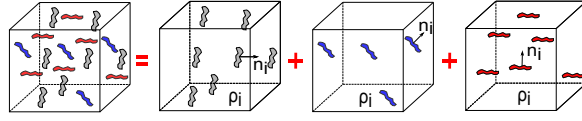Tensors $\underline{\underline{N}}_i$ are fixed and do not evolve along with the loading. They must fulfill these two

Figure 1: Crack families of normal $\underline{n}_i$ and density ρ_i

conditions :

- any tensor $\underline{n}_i \otimes \underline{n}_i$ is an additive combination of $\underline{\underline{N}}_i$,

- an isotropic damage state must be described by a constant crack density ρ_0 in each direction $\underline{\underline{N}}_i : \sum_i \rho_i \underline{\underline{N}}_i \propto \rho_0 \underline{1}$ where $\underline{1}$ is the second-order identity tensor.

Nine directionnal tensors are defined in order to fulfill the previous conditions. Their orientation depends on the loading configuration. In the orthonormal basis $(\underline{e}_1, \underline{e}_2, \underline{e}_3)$, they are expressed as follows:

$$\underline{\underline{N}}_1 = \underline{e}_1 \otimes \underline{e}_1 \quad \underline{\underline{N}}_2 = \underline{e}_2 \otimes \underline{e}_2 \quad \underline{\underline{N}}_3 = \underline{e}_3 \otimes \underline{e}_3$$
$$\underline{\underline{N}}_4 = (\underline{e}_1 + \underline{e}_2) \otimes (\underline{e}_1 + \underline{e}_2) \quad \underline{\underline{N}}_5 = \tfrac{1}{2}(\underline{e}_1 + \underline{e}_3) \otimes (\underline{e}_1 + \underline{e}_3) \quad \underline{\underline{N}}_6 = \tfrac{1}{2}(\underline{e}_2 + \underline{e}_3) \otimes (\underline{e}_2 + \underline{e}_3)$$
$$\underline{\underline{N}}_7 = \tfrac{1}{2}(\underline{e}_1 - \underline{e}_2) \otimes (\underline{e}_1 - \underline{e}_2) \quad \underline{\underline{N}}_8 = \tfrac{1}{2}(\underline{e}_1 - \underline{e}_3) \otimes (\underline{e}_1 - \underline{e}_3) \quad \underline{\underline{N}}_9 = \tfrac{1}{2}(\underline{e}_2 - \underline{e}_3) \otimes (\underline{e}_2 - \underline{e}_3)$$

It is important to highlight that the nine crack families do not interact. Each associated microcracking density ρ_i is considered as an internal variable.

2.2 Constitutive laws

This model is expressed within the framework of the irreversible processes thermodynamics. The constitutive laws are written following the approach of Bargellini [7]. Under the hypothesis of non-interacting cracks, no residual strains and neglecting friction on the crack lips, the Helmholtz free energy expression is given by equation 2.

$$
\begin{aligned}
\psi(\rho, \underline{\underline{N}}, \underline{\underline{\epsilon}}, z) = \psi_0 \;+\; & \sum_{i=1}^{9} \rho_i [\alpha[tr(\underline{\underline{\epsilon}} \cdot \underline{\underline{\epsilon}}) - \frac{1}{2}tr^2(\underline{\underline{\epsilon}}) + tr(\underline{\underline{\epsilon}})tr(\underline{\underline{\epsilon}} \cdot \underline{\underline{N}}_i)] \\
+\; & 2\beta tr(\underline{\underline{\epsilon}} \cdot \underline{\underline{\epsilon}} \cdot \underline{\underline{N}}_i) \\
-\; & (\frac{3}{2}\alpha + 2\beta)tr^2(\underline{\underline{\epsilon}} \cdot \underline{\underline{N}}_i)H(-tr(\underline{\underline{\epsilon}} \cdot \underline{\underline{N}}_i))] \\
+\; & \sum_{i=1}^{9} \mathrm{H}_i(z_i)
\end{aligned}
\tag{2}
$$

where ψ_0 is the elastic free energy, $\mathrm{H}_i(z_i)$ the consolidation function depending on the hardening variable z_i; $tr(\cdot)$ is the trace of $(\cdot)$; $H(\cdot)$ is the Heaviside function and α, β two material parameters $(\alpha, \beta < 0)$. Crack closure effect is taken into account by means of an opening/closure condition given by equation 3.

$$\underline{\underline{N}}_i : \underline{\underline{\epsilon}} = tr(\underline{\underline{\epsilon}} \cdot \underline{\underline{N}}_i) \leq 0 \tag{3}$$

The stress-strain response is obtained by derivation of the free energy with respect to $\underline{\epsilon}$. The state law is expressed as follows:

$$
\begin{aligned}
\underline{\underline{\sigma}}(\rho, \underline{\underline{N}}, \underline{\underline{\epsilon}}) = \frac{\partial \psi}{\partial \underline{\underline{\epsilon}}} = \underline{\underline{\sigma}}_0 \quad &+ \quad \sum_{i=1}^{9} \rho_i [\alpha[2\underline{\underline{\epsilon}} - tr(\underline{\underline{\epsilon}})\underline{\underline{1}} + tr(\underline{\underline{\epsilon}})\underline{\underline{N}}_i + tr(\underline{\underline{\epsilon}} \cdot \underline{\underline{N}}_i)\underline{\underline{1}}] \\
&+ \quad 2\beta(\underline{\underline{\epsilon}} \cdot \underline{\underline{N}}_i + \underline{\underline{N}}_i \cdot \underline{\underline{\epsilon}}) \\
&- \quad (3\alpha + 4\beta)tr(\underline{\underline{\epsilon}} \cdot \underline{\underline{N}}_i)\underline{\underline{N}}_i H(-tr(\underline{\underline{\epsilon}} \cdot \underline{\underline{N}}_i))]
\end{aligned}
\tag{4}
$$

where $\underline{\underline{\sigma}}_0 = \dfrac{\partial \psi_0}{\partial \underline{\underline{\epsilon}}}$. We define, for sake of simplicity, $g_i(\underline{\underline{x}}, \underline{\underline{N}}_i) :\overset{\text{def}}{=} \alpha[2\underline{\underline{x}} - tr(\underline{\underline{x}})\underline{\underline{1}} + tr(\underline{\underline{x}})\underline{\underline{N}}_i + tr(\underline{\underline{x}} \cdot \underline{\underline{N}}_i)\underline{\underline{1}}] + 2\beta(\underline{\underline{x}} \cdot \underline{\underline{N}}_i + \underline{\underline{N}}_i \cdot \underline{\underline{x}}) - (3\alpha + 4\beta)tr(\underline{\underline{x}} \cdot \underline{\underline{N}}_i)\underline{\underline{N}}_i H(-tr(\underline{\underline{x}} \cdot \underline{\underline{N}}_i))$ linear with respect to $\underline{\underline{x}}$ which verifies the following properties $g_i(\underline{\underline{0}}, \underline{\underline{N}}_i) = \underline{\underline{0}}$ and $g_i(\lambda \underline{\underline{x}}, \underline{\underline{N}}_i) = \lambda g_i(\underline{\underline{x}})$. Derivation of the free energy with respect to the internal variables ρ_i, z_i gives the associated thermodynamic forces F^{ρ_i} and the hardening function $Z_i(z_i)$ respectively. The threshold surface is:

$$
\phi_i = F^{\rho_i} - (Z_0 + Z_i(z_i))
\tag{5}
$$

where $F^{\rho_i} = -(\frac{3}{2}\alpha + 2\beta)tr^2(\underline{\underline{\epsilon}} \cdot \underline{\underline{N}}_i)(1 - H(-tr(\underline{\underline{\epsilon}} \cdot \underline{\underline{N}}_i)))$; Z_0 is an initial threshold function of the elastic limit σ_u and the Young modulus E and $Z_i(z_i) = Z_0(e^{-z_i/C_3^{\rho_i}} - 1)$ where $C_3^{\rho_i}$ is a material parameter $(C_3^{\rho_i} > 0)$. The main assumption of the model is that cracks evolve only when they are open. Furthermore, if the loading direction changes, crack densities will follow this evolution given the fact that thermodynamic forces depend on the current strain. The flow rule for the microcracking densities is obtained by the threshold surface and the consistency conditions.

$$
\rho_i = C_3^{\rho_i} \, ln\left(\frac{F^{\rho_i}}{Z_0}\right) \quad \rho_i \in [0; \rho_{i,max}]
\tag{6}
$$

3 EMBEDDED DISPLACEMENT DISCONTINUITY FRAMEWORK

In this section the embedded kinematics is exposed. Then, the anisotropic damage model presented in section 2, is enriched and a regularization of the Dirac distribution is performed. The main features of the method are highlighted.

3.1 Kinematics

Consider a Kirchhoff plate Ω of thickness h defined by a normal $\underline{e}_z$. The displacement field is given by equation 7.

$$
\underline{u}(\underline{x}, t) = \underline{u}_t(\underline{x}, t) + z \, \underline{\theta}(\underline{x}, t) \wedge \underline{e}_z
\tag{7}
$$

where $\underline{u}_t(\underline{x}, t)$ is the displacement vector and $\underline{\theta}(\underline{x}, t)$ the rotation vector. Let Γ_S be the discontinuity surface which splits the body into two parts Ω^- and Ω^+. Let $\underline{n}$ be the normal to the discontinuity pointing to Ω^+.

In this paper, only the membrane part of the kinematics $\underline{u}_t$ is enriched with a displacement jump as given in equation 8.

$$
\underline{u}_t(\underline{x}, t) = \overline{\underline{u}}(\underline{x}, t) + H_{\Gamma_S}(\underline{x})[\![\underline{u}]\!](\underline{x}, t)
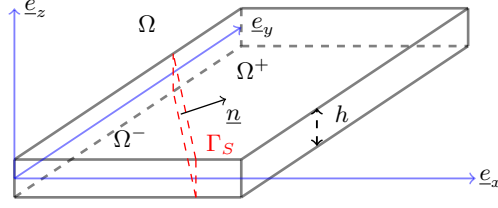\tag{8}
$$

Figure 2: Discontinuity surface Γ_s inside the plate Ω

where $\overline{u}(x,t)$ [1] stands for the regular continuous displacement field and $[\![u]\!](x,t)$ is the discontinuity jump through Γ_S. The classical Heaviside function is $H_{\Gamma_S}(\underline{x}) = 1$ if $\underline{x} \in \Omega^+$ and 0 otherwise. The strain field obtained from the symmetric gradient of the displacement field is given by equation 9.

$$\underline{\underline{\epsilon}} = \underbrace{\nabla^s \overline{\underline{u}} + H_{\Gamma_S}(\underline{x})\nabla^s[\![\underline{u}]\!]}_{\text{continuous bounded}} + \underbrace{\delta_{\Gamma_S}([\![\underline{u}]\!] \otimes \underline{n})^s}_{\text{discontinuous unbounded}} = \overline{\underline{\underline{\epsilon}}} + \delta_{\Gamma_S}([\![\underline{u}]\!] \otimes \underline{n})^s \tag{9}$$

where $(.)^s$ is the symmetric part of $(.)$ and δ_{Γ_S} is the Dirac distribution on Γ_S. The strain field is composed of a continuous and bounded part and a singular unbounded one.

Following the approach of Oliver [8], the Dirac distribution is approximated by a regularization function $\delta_{\Gamma_S}^k(\underline{x})$ defined as follows:

$$\delta_{\Gamma_S}^k(\underline{x}) = \frac{1}{k}\mu_{\Gamma_S^k}(\underline{x}) \tag{10}$$

with $\mu_{\Gamma_S^k}(\underline{x}) = 1$ if $\underline{x} \in \Gamma_S^k$ and 0 otherwise, where Γ_S^k is a discontinuity band of bandwidth k as small as possible such that, $\lim_{k \to 0} \delta_{\Gamma_S}^k(\underline{x}) = \delta_{\Gamma_S}(\underline{x})$.

3.2 Strong discontinuity framework

In the strong discontinuity regime, the regularized version of the strain field is :

$$\underline{\underline{\epsilon}} = \overline{\underline{\underline{\epsilon}}} + \delta_{\Gamma_S}([\![\underline{u}]\!] \otimes \underline{n})^s \approx \overline{\underline{\underline{\epsilon}}} + \frac{1}{k}([\![\underline{u}]\!] \otimes \underline{n})^s \tag{11}$$

3.2.1 Discrete hardening law

The traction continuity conditions at the interface Γ_S and in the domain $\Omega \backslash \Gamma_S$, impose bounded values of the traction vector components and the stress tensor even if strains are not bounded. At the onset of the discontinuity, stresses in the rate form considering equations 11 and 4, where the non-linear part is replaced by a function $g(\underline{\underline{\epsilon}}, \underline{\underline{N}}_i)$ for sake of simplicity, are expressed as follows:

$$\underline{\underline{\dot{\sigma}}}_{\Gamma_S} = \mathbb{C} : (\dot{\overline{\underline{\underline{\epsilon}}}} + \frac{1}{k}([\![\dot{\underline{u}}]\!] \otimes \underline{n})^s) + \sum_{i=1}^{9} \dot{\rho}_i g_i(\overline{\underline{\underline{\epsilon}}} + \frac{1}{k}([\![\underline{u}]\!] \otimes \underline{n})^s, \underline{\underline{N}}_i) + \sum_{i=1}^{9} \rho_i g_i(\dot{\overline{\underline{\underline{\epsilon}}}} + \frac{1}{k}([\![\dot{\underline{u}}]\!] \otimes \underline{n})^s, \underline{\underline{N}}_i)$$

where $\mathbb{C}$ is the Hooke's tensor. Taking the limit of $k\underline{\underline{\dot{\sigma}}}_{\Gamma_S}$ when k tends to 0 gives:

---

[1]The notation $(\underline{x}, t)$ will be omitted for easy reading

$$\lim_{k \to 0} k\dot{\underline{\underline{\sigma}}}_{\Gamma_S} = \mathbb{C} : (\llbracket \underline{\dot{u}} \rrbracket \otimes \underline{n})^s + \sum_{i=1}^{9} \dot{\rho}_i g_i((\llbracket \underline{u} \rrbracket \otimes \underline{n})^s, \underline{\underline{N}}_i) + \sum_{i=1}^{9} \rho_i g_i((\llbracket \underline{\dot{u}} \rrbracket \otimes \underline{n})^s, \underline{\underline{N}}_i) \quad (12)$$

Equation 12 is equal to 0 because $\dot{\underline{\underline{\sigma}}}_{\Gamma_S}$ is bounded on Γ_S. Furthermore, equation 12 translates that the evolution of the discontinuty jump rate $\llbracket \underline{\dot{u}} \rrbracket$ is a function of $\dot{\rho}_i, \rho_i, \underline{n}_i$. Then, the discontinuty jump rate is bounded on Γ_S if $\dot{\rho}_i$ is bounded. The flow rules give:

$$\begin{cases} \dot{\rho}_i = \dot{\lambda}_i \dfrac{\partial \phi_i}{\partial F^{\rho_i}} = \dot{\lambda}_i \\ \dot{z}_i = \dot{\lambda}_i \dfrac{\partial \phi_i}{\partial Z_i} = -\dot{\lambda}_i \end{cases} \Rightarrow \dot{\rho}_i = -\dot{z}_i \quad (13)$$

where $\dot{\lambda}_i$ are the plastic multipliers. Considering the consistency condition $\dot{\lambda}\dot{\phi}_i = 0$ at the interface Γ_S and the flow rules given by equation 13, one obtains:

$$- (3\alpha + 4\beta) tr((\underline{\underline{\bar{\varepsilon}}} + \frac{1}{k}(\llbracket \underline{u} \rrbracket \otimes \underline{n})^s) \cdot \underline{\underline{N}}_i)(1 - H(tr((\underline{\underline{\bar{\varepsilon}}} + \frac{1}{k}(\llbracket \underline{u} \rrbracket \otimes \underline{n})^s) \cdot \underline{\underline{N}}_i)))\underline{\underline{N}}_i : (\dot{\underline{\underline{\bar{\varepsilon}}}} + \frac{1}{k}(\llbracket \underline{\dot{u}} \rrbracket \otimes \underline{n})^s)$$
$$+ \mathcal{H}_i \dot{\rho}_i = 0 \quad (14)$$

where $\mathcal{H}_i = \dfrac{\partial Z_i(z_i)}{\partial z_i} = \dfrac{\partial^2 H_i(z_i)}{\partial^2 z_i}$ is the hardening parameter. Taking the limit of $k\dot{\rho}_i$ when k tends to 0 yields:

$$\lim_{k \to 0} k\dot{\rho}_i = \frac{1}{\mathcal{H}_i}(3\alpha + 4\beta)tr((\llbracket \underline{u} \rrbracket \otimes \underline{n})^s \cdot \underline{\underline{N}}_i)(1 - H(tr((\llbracket \underline{u} \rrbracket \otimes \underline{n})^s \cdot \underline{\underline{N}}_i)))\underline{\underline{N}}_i : (\llbracket \underline{\dot{u}} \rrbracket \otimes \underline{n})^s :\overset{\text{def}}{=} \dot{\bar{\rho}}_i \quad (15)$$

We can define $\dot{\bar{\lambda}} = \lim_{k \to 0}(k\dot{\lambda})$ the discrete plastic multiplier and $\dot{\bar{\rho}}_i = \lim_{k \to 0}(k\dot{\rho}_i)$ (respectively $\dot{\bar{z}}_i = \lim_{k \to 0}(k\dot{z}_i)$) the discrete microcracking variables (respectively the discrete hardening variables). The hardening function rate is then $\dot{Z}_i = -\mathcal{H}_i\dot{\rho}_i = -\mathcal{H}_i\dfrac{\dot{\bar{\rho}}_i}{k} = -\dfrac{\mathcal{H}_i}{k}\dot{\bar{\rho}}_i = -\overline{\mathcal{H}_i}\dot{\bar{\rho}}_i$ with $\overline{\mathcal{H}_i}$ the discrete hardening parameter. The discrete microcrack densities rate $\dot{\bar{\rho}}_i$ is bounded on Γ_S and so is the displacement jump rate.

3.2.2 Discrete free energy

Considering the regularized strain field, the free energy is expressed as follows:

$$\psi_{\Gamma_S} = \psi_0 + \sum_{i=1}^{9} \rho_i[\alpha[tr((\underline{\underline{\bar{\varepsilon}}} + \frac{1}{k}(\llbracket \underline{u} \rrbracket \otimes \underline{n})^s) \cdot (\underline{\underline{\bar{\varepsilon}}} + \frac{1}{k}(\llbracket \underline{u} \rrbracket \otimes \underline{n})^s)) - \frac{1}{2}tr^2((\underline{\underline{\bar{\varepsilon}}} + \frac{1}{k}(\llbracket \underline{u} \rrbracket \otimes \underline{n})^s))$$
$$+ tr((\underline{\underline{\bar{\varepsilon}}} + \frac{1}{k}(\llbracket \underline{u} \rrbracket \otimes \underline{n})^s))tr((\underline{\underline{\bar{\varepsilon}}} + \frac{1}{k}(\llbracket \underline{u} \rrbracket \otimes \underline{n})^s) \cdot \underline{\underline{N}}_i)]$$
$$+ 2\beta tr((\underline{\underline{\bar{\varepsilon}}} + \frac{1}{k}(\llbracket \underline{u} \rrbracket \otimes \underline{n})^s) \cdot (\underline{\underline{\bar{\varepsilon}}} + \frac{1}{k}(\llbracket \underline{u} \rrbracket \otimes \underline{n})^s) \cdot \underline{\underline{N}}_i)$$
$$- (\frac{3}{2}\alpha + 2\beta)tr^2((\underline{\underline{\bar{\varepsilon}}} + \frac{1}{k}(\llbracket \underline{u} \rrbracket \otimes \underline{n})^s) \cdot \underline{\underline{N}}_i)H(-tr((\underline{\underline{\bar{\varepsilon}}} + \frac{1}{k}(\llbracket \underline{u} \rrbracket \otimes \underline{n})^s) \cdot \underline{\underline{N}}_i))]$$
$$+ \sum_{i=1}^{9} H_i(\bar{z}_i) \quad (16)$$

The derivative of equation 16 with respect to the discontinuity jump gives:

$$\frac{\partial \psi_{\Gamma_S}}{\partial [\![u]\!]} = \frac{\partial \psi_{\Gamma_S}}{\partial \underline{\underline{\epsilon}}} : \frac{\partial \underline{\underline{\epsilon}}}{\partial [\![u]\!]} = \underline{\underline{\sigma}}_{\Gamma_S} : \frac{1}{k}(\underline{\underline{1}} \otimes \underline{n})^s = \frac{1}{k}\underline{\underline{\sigma}}_{\Gamma_S} \cdot \underline{n} = \frac{1}{k}\underline{t}_{\Gamma_S} \tag{17}$$

Taking the limit of equation 17 yields $\underline{t}_{\Gamma_S} = \lim\limits_{k\to 0} k \dfrac{\partial \psi_{\Gamma_S}}{\partial [\![u]\!]} = \dfrac{\partial \lim\limits_{k\to 0} k\psi_{\Gamma_S}}{\partial [\![u]\!]} = \dfrac{\partial \overline{\psi}_{\Gamma_S}}{\partial [\![u]\!]}$ where $\overline{\psi}_{\Gamma_S}$ is the discrete free energy at the discontinuity interface. Discrete thermodynamic forces $\overline{F}^{\overline{\rho}_i}$ are obtained immediately by derivation of the discrete free energy with respect to the discrete microcrack densities variables.

3.2.3 Continuum-discrete equivalence

At the onset of localization, the threshold surface is zero so the stresses reach the elastic limit σ_u, the thermodynamic forces reach the intial threshold value Z_0 and the elastic free energy is equal to a constant value depending on the elastic limit ψ_u. The discrete model obtained considering the previous developments can be summarized as follows:

Free energy

$$\overline{\psi}_{\Gamma_S} = \sum_{i=1}^{9} \overline{\rho}_i [\alpha[tr(([\![u]\!] \otimes \underline{n})^s \cdot ([\![u]\!] \otimes \underline{n})^s) - \frac{1}{2}tr^2(([\![u]\!] \otimes \underline{n})^s) + tr(([\![u]\!] \otimes \underline{n})^s)tr(([\![u]\!] \otimes \underline{n})^s \cdot \underline{\underline{N}}_i)]$$

$$+ 2\beta tr(([\![u]\!] \otimes \underline{n})^s \cdot ([\![u]\!] \otimes \underline{n})^s \cdot \underline{\underline{N}}_i) - (\frac{3}{2}\alpha + 2\beta)tr^2(([\![u]\!] \otimes \underline{n})^s \cdot \underline{\underline{N}}_i)H(-tr(([\![u]\!] \otimes \underline{n})^s \cdot \underline{\underline{N}}_i))]$$

$$+ \sum_{i=9}^{9} \mathrm{H}_i(\overline{z}_i) \qquad \text{with} \quad \psi_{\Gamma_S} \in [\psi_u, \infty[\tag{18}$$

Traction vector

$$\underline{t}_{\Gamma_S} = \frac{\partial \overline{\psi}_{\Gamma_S}}{\partial [\![u]\!]} = \sum_{i=1}^{9} \overline{\rho}_i g_i(([\![u]\!] \otimes \underline{n})^s, \underline{\underline{N}}_i) \cdot \underline{n} \quad \text{with} \quad \|\underline{t}_{\Gamma_S}\| \in [\sigma_u, 0[\tag{19}$$

Thermodynamic forces

$$\overline{F}^{\overline{\rho}_i} = -\frac{\partial \overline{\psi}_{\Gamma_S}}{\partial \overline{\rho}_i}$$

$$= -(\frac{3}{2}\alpha + 2\beta)tr^2(([\![u]\!] \otimes \underline{n})^s \cdot \underline{\underline{N}}_i)(1 - H(-tr(([\![u]\!] \otimes \underline{n})^s \cdot \underline{\underline{N}}_i))) \quad \text{with} \quad \overline{F}^{\overline{\rho}_i} \in [0, \overline{Z}_i] \tag{20}$$

Hardening function

$$\overline{Z}_i = \frac{\partial \overline{\psi}_{\Gamma_S}}{\partial \overline{z}_i} \quad \text{with} \quad \overline{Z}_i \in [\frac{\sigma_u}{2E}, 0[\tag{21}$$

Microcrack densities

$$\overline{\rho}_i = C_3^{\rho_i} \ln\left(\frac{\overline{F}^{\overline{\rho}_i}}{Z_0}\right) \qquad \text{with} \quad \overline{\rho}_i \in]-\infty; \overline{\rho}_{i,max}] \tag{22}$$

The following one to one correspondance of the continuum damage model and the induced enriched one is given in table 1.

Table 1: Correspondance of the continuum and the enriched model

Continuum	ψ	$\underline{\underline{\sigma}}$	$\underline{\underline{\epsilon}}$	F^{ρ_i}	ρ_i	$Z_i(z_i)$
Enriched	$\overline{\psi}_{\Gamma_S}$	$\underline{t}_{\Gamma_S}$	$[\![\underline{u}]\!]$	$\overline{F}^{\overline{\rho}_i}$	$\overline{\rho}_i$	$\overline{Z}_i(\overline{z}_i)$

4 NUMERICAL PROCEDURE

In this section, the numerical aspects are discussed. The enriched model has been implemented in the finite element code Cast3M [9]. The local integration algorithm is also presented.

4.1 Embedded Finite Element Method

For numerical simulations the Embedded Finite Element Method is used. This method consists in adding a degree of freedom locally in the element that is crossed by the crack (see figure 3). The displacement field is written as:

$$\underline{u} = \sum_{i \in I} \underline{u}_i \phi_i + \sum_{e \in E} \beta_e M^e_{\Gamma_S} \tag{23}$$

with $M^e_{\Gamma_S} = H_{\Gamma_S} - \varphi^e$ and $\varphi^e = \sum_{i=1}^{n^e_{node+}} \phi^e_i$, where E is the set of elements to be enriched, n^e_{node+} are the nodes of element e in Ω^+, β_e are the degrees of freedom accounting for the jump and $M^e_{\Gamma_S}$ is the jump shape function such that $M^e_{\Gamma_S} = 1$ in the discontinuity and 0 otherwise.
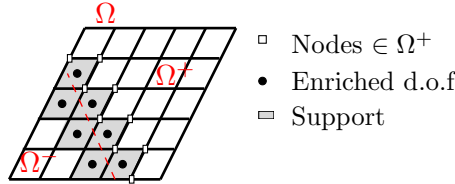
Figure 3: Elemental enrichment E-FEM

The inherent local character of the method reduces calculation time. Indeed, for fixed displacements a local equation solving is performed and then the local information (displacement jump) is condensed within the finite element for global resolution (global displacements). Hence, global system size remains unchanged and the structure of the element code too.

4.2 Local integration algorithm

The local integration algorithm for the numerical procedure is given in figure 4.

5 NUMERICAL APPLICATIONS

In this section numerical simulations on the integration point level and a three-point bending test carried out on a single edge notched specimen are emphasized.

Beginning of the time step t, updating strains $\underline{\underline{\epsilon}}^{t+\Delta t} = \underline{\underline{\epsilon}}^{t} + \Delta \underline{\underline{\epsilon}}$.
The known variables are:
$\underline{\underline{\sigma}}^{t,0}, \underline{t}^{t,0} = \underline{\underline{\sigma}}^{t,0} \cdot \underline{n}, F^{t,0}, \overline{Z}_i^{t,0}, [\![\underline{u}]\!]^{t,0}, \overline{\rho}_i^{t,0}, \underline{t}_{\Gamma_S}^{t,0}$

Updating stresses, thermodynamic forces:
$\underline{\underline{\sigma}}^{t+\Delta t,0}, \underline{t}^{t+\Delta t,0}, F^{t+\Delta t,0}$
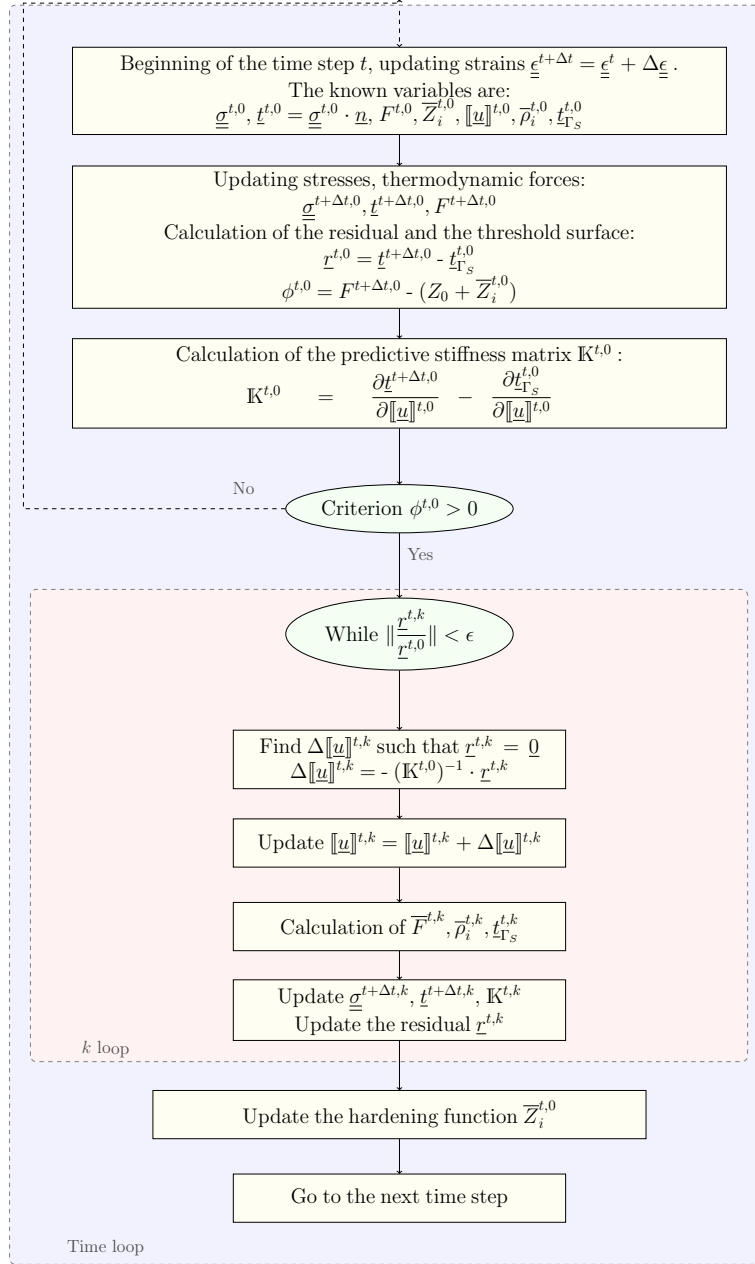Calculation of the residual and the threshold surface:
$\underline{r}^{t,0} = \underline{t}^{t+\Delta t,0} - \underline{t}_{\Gamma_S}^{t,0}$
$\phi^{t,0} = F^{t+\Delta t,0} - (Z_0 + \overline{Z}_i^{t,0})$

Calculation of the predictive stiffness matrix $\mathbb{K}^{t,0}$:
$\mathbb{K}^{t,0} \quad = \quad \dfrac{\partial \underline{t}^{t+\Delta t,0}}{\partial [\![\underline{u}]\!]^{t,0}} \quad - \quad \dfrac{\partial \underline{t}_{\Gamma_S}^{t,0}}{\partial [\![\underline{u}]\!]^{t,0}}$

No

Criterion $\phi^{t,0} > 0$

Yes

While $\|\dfrac{\underline{r}^{t,k}}{\underline{r}^{t,0}}\| < \epsilon$

Find $\Delta [\![\underline{u}]\!]^{t,k}$ such that $\underline{r}^{t,k} = \underline{0}$
$\Delta [\![\underline{u}]\!]^{t,k} = - (\mathbb{K}^{t,0})^{-1} \cdot \underline{r}^{t,k}$

Update $[\![\underline{u}]\!]^{t,k} = [\![\underline{u}]\!]^{t,k} + \Delta [\![\underline{u}]\!]^{t,k}$

Calculation of $\overline{F}^{t,k}, \overline{\rho}_i^{t,k}, \underline{t}_{\Gamma_S}^{t,k}$

Update $\underline{\underline{\sigma}}^{t+\Delta t,k}, \underline{t}^{t+\Delta t,k}, \mathbb{K}^{t,k}$
Update the residual $\underline{r}^{t,k}$

k loop

Update the hardening function $\overline{Z}_i^{t,0}$

Go to the next time step

Time loop

Figure 4: Local integration algorithm

5.1   Gauss point results

The results of a cyclic tension/compression test at the integration point level are reported in figure 5. The material parameters used for this simulation are given in table 2.

The softening behaviour of concrete is well reproduced, as expected. The choice of a linear

Table 2: Material parameter for the integration point level test

Parameter	E	ν	α	β	Z_0	$C_3^{\rho_1}$	$C_3^{\rho_{4,5,7,8}}$
Value	29 GPa	0.21	-12.5 GPa	-14.5 GPa	420 MPa	0.05	0.01

behaviour in compression has been made. The correspondance between the continuous model and the enriched one is emphasized. The enriched model depicts the softening behaviour in terms of traction vector-displacement jump. Elastic properties are totally recovered in compression. The anisotropy of the model is emphasized by the evolution of microcracking densities. Uniaxial traction in direction 1 enables activation of two microcracking groups : cracks normal to the loading ρ_1 and other microckracks $\rho_{4,5,7,8}$ which evolve slower.
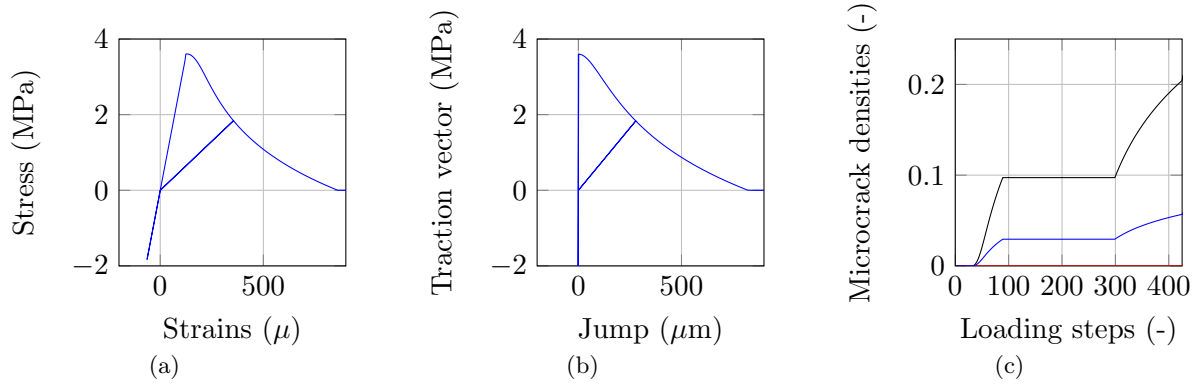

Figure 5: Continuum model 5(a), traction-displacement jump evolution 5(b), microcrack densities evolution (ρ_1, $\rho_{4,5,7,8}$, $\rho_{2,3,6,9}$) 5(c)

5.2 Three-point bending test

A three-point bending test campaign on mortar beams, undergone in the LMT Cachan, is used [1]. Square section specimens of dimension $D = 70$ cm and length $4D$ have been tested. A single notch of depth $D/2$ and thickness 3 mm was sawed at the center of the specimen before the test. The geometry and the boundary conditions are given in figure 6. The material parameter used for this test are given in table 3.

Table 3: Material parameter for the three-point bending test

Parameter	E	ν	α	β	Z_0	$C_3^{\rho_1}$	$C_3^{\rho_{4,5,7,8}}$
Value	34 GPa	0.21	-14.33 GPa	-14.29 GPa	195 MPa	1.56	0.05

The global results in terms of load-deflexion given by the model are compared with the experimental results and are reported in figure 7(a). A good agreement with the experiment is obtained. In order to illustrate the performances of the model at capturing local information
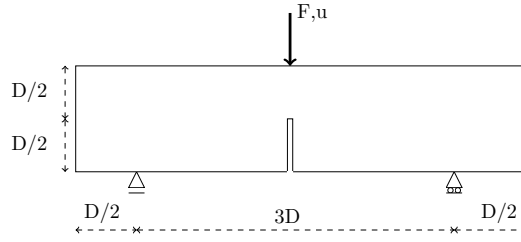
Figure 6: Geometry and boundary conditions of the three-point bending test

like crack openings, the evolution of the height of the specimen versus crack opening is reported in figure 7(b). Results are given for different loading levels - at peak, 75% post-peak and 50% post-peak. The model is able to capture quite well the local behaviour as well as the overall behaviour.
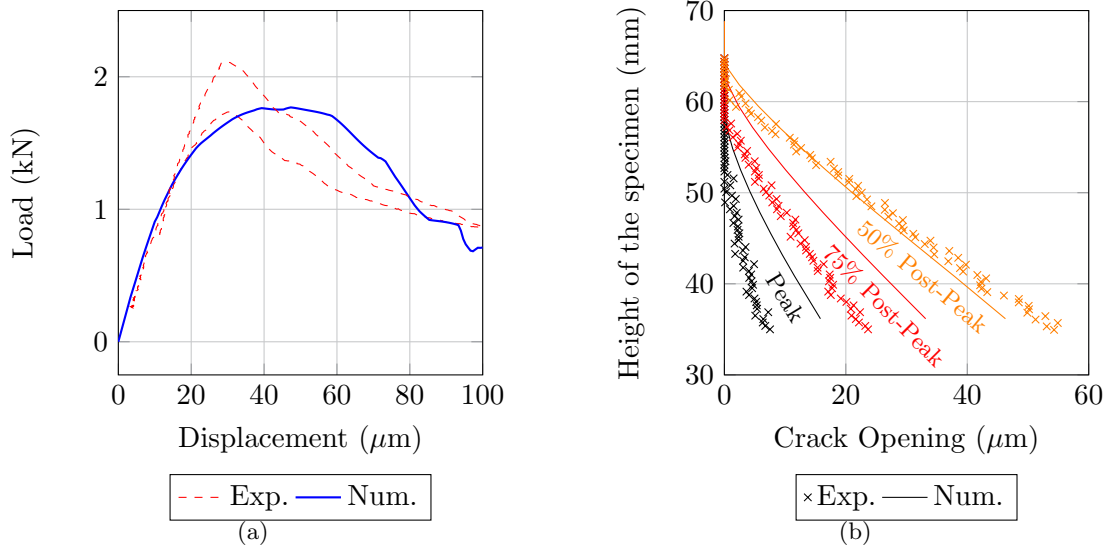

Figure 7: Numerical model compared to experiment: load deflexion response 7(a), crack openings 7(b)

6   CONCLUSIONS

In this paper, an enriched plate-formulation was presented. The developed model is based on an anisotropic damage model for quasi-brittle materials. The damage state is expressed as the contribution of nine crack families of normal $\underline{n}_i$ and density $\underline{\rho}_i$. The model can represent either mode I and mode II cracking mechanisms, accounts for different crack orientations and crack closure effect. The strong discontinuity approach was used to capture localisation features like crack openings. A regularized version of the Dirac distribution and the hardening parameter allows for the establishment of an enriched model compatible with the continuous one. The E-FEM technique is efficient, non intrusive for the finite element code and it is not time-consuming. Simulations at the integration point level and a three-point bending test carried out on a single

344

edge notched beam have shown the performance of the model. Global and local information are well captured. Results presented in this paper constitute the first step for futher development. Further simulations will be performed on reinforced concrete elements, like reinforced concrete ties and shear walls, to show the performances of our work. An identification procedure for the material parameters of the damage model is under development. Virtual testing based on a *lattice* element method is used as a reference model. An optimisation method based on the trust region effective algorithm is considered for the identification procedure. The next step of our work is the full enrichment of the plate kinematics - the flexional part of the kinematics will also be enriched with the same technique. Therefore, the double enhancedd model would represent complex failure behaviour of reinforced concrete components.

REFERENCES

[1] Oliver-Leblond, C., Delaplace, A., Ragueneau, F. and Richard, B. Non-intrusive global/local analysis for the study of fine cracking. *International Journal for Numerical and Analytical Methods in Geomechanics* (2013) **37(8)**, 973–992.

[2] Jirásek, M. and Zimmermann, T. Analysis of rotating crack model. *Journal of engineering mechanics* (1998) **124(8)**:842–851.

[3] Welemane, H. and Cormery, F. Some remarks on the damage unilateral effect modelling for microcracked materials. *International Journal of Damage Mechanics* (2002) **11(1)**:65–86.

[4] Carol, I. and Willam, K. Spurious energy dissipation/generation in stiffness recovery models for elastic degradation and damage. *International Journal of Solids and Structures* (1996) **33(20)**:2939–2957.

[5] Oliver, J. Modelling strong discontinuities in solid mechanics via strain softening constitutive equations. Part 1 : Fundamentals and Part 2: Numerical simulation. *International Journal for Numerical Methods in Engineering* (1996) **39(21)**: 3575-3623.

[6] Sukumar, N., Moës, N., Moran, B. and Belytschko, T. Extended finite element method for threedimensional crack modelling. *International Journal for Numerical Methods in Engineering* (2000) **48(11)**:1549–1570.

[7] Bargellini, R., Halm, D. and Dragon, A. Modelling of quasi-brittle behaviour: a discrete approach coupling anisotropic damage growth and frictional sliding. *European Journal of Mechanics-A/Solids* (2008) **27(4)**:564-581.

[8] Oliver, J. On the discrete constitutive models induced by strong discontinuity kinematics and continuum constitutive equations. *International Journal of Solids and Structures* (2000) **37(48)**:7207-7229.

[9] www.cast3m-cea.fr